Accepted Manuscript

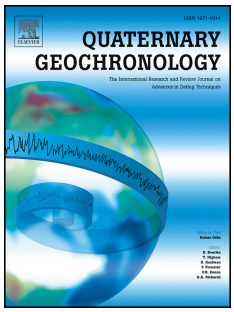

pIRIR and IR-RF dating of archaeological deposits at Badahlin and Gu Myaung Caves – First luminescence ages for Myanmar

Maria Schaarschmidt, Xiao Fu, Bo Li, Ben Marwick, Kyaw Khaing, Katerina Douka, Richard G. Roberts

PII: S1871-1014(17)30240-6

DOI: 10.1016/j.quageo.2018.01.001

Reference: QUAGEO 886

To appear in: *Quaternary Geochronology*

Received Date: 6 December 2017

Revised Date: 20 December 2017

Accepted Date: 4 January 2018

Please cite this article as: Schaarschmidt, M., Fu, X., Li, B., Marwick, B., Khaing, K., Douka, K., Roberts, R.G., pIRIR and IR-RF dating of archaeological deposits at Badahlin and Gu Myaung Caves – First luminescence ages for Myanmar, *Quaternary Geochronology* (2018), doi: 10.1016/j.quageo.2018.01.001.

pIRIR and IR-RF dating of archaeological deposits at Badahlin and Gu Myaung Caves – first luminescence ages for Myanmar

Maria Schaarschmidt[a*], Xiao Fu[a], Bo Li[a], Ben Marwick[a,b], Kyaw Khaing[c], Katerina Douka[d], Richard G. Roberts[a,e]

[a] Centre for Archaeological Science, School of Earth and Environmental Sciences, University of Wollongong, Wollongong, NSW 2522, Australia

[b] Department of Anthropology, University of Washington, Seattle, WA 98195, USA

[c] Field School of Archaeology, Pyay, Department of Archaeology and National Museum, Ministry of Religious Affairs and Culture, Myanmar

[d] Research Laboratory for Archaeology and the History of Art, University of Oxford, Oxford OX1 3QY, UK

[e] ARC Centre of Excellence for Australian Biodiversity and Heritage, University of Wollongong, Wollongong, NSW 2522, Australia

* Corresponding author: ms648@uowmail.edu.au

Abstract

Reliable chronologies are essential for understanding the timing and routes of human dispersal through Southeast Asia, both of which remain open questions. This study provides luminescence chronologies for two archaeological sites in Myanmar—Badahlin Cave and Gu Myaung Cave—from which Palaeolithic artefacts have been recovered. We applied single-grain post-infrared infrared stimulated luminescence (pIRIR) and multi-grain infrared-radiofluorescence (IR-RF) dating methods to potassium-rich feldspar (K-feldspar) grains extracted from the sedimentary deposits at these two sites. Luminescence characteristics of the K-feldspar extracts showed that the procedures were well suited for dating. The single-grain pIRIR ages indicate human occupation of Badahlin and Gu Myaung Caves by around ~29—30 ka and ~25—27 ka, respectively. We obtained age overestimates using the IR-RF dating signal compared to pIRIR dating, which we attribute to insufficient bleaching of the IR-RF signal at the time of sediment deposition and a, so far, unknown residual dose.

***Keywords**: K-feldspar, single-grain post-IR IRSL, radiofluorescence, anomalous fading, Southeast Asia*

1 Introduction

Badahlin and Gu Myaung Caves both lie at the foot of the Shan Plateau, which stretches eastward from central Myanmar into northern Thailand (Fig. 1). Badahlin Cave was first excavated in 1969 (Aung Thaw, 1971) when stone artefacts and animal bones were recovered. Radiocarbon (^{14}C) dating indicated a maximum age for the cultural materials of ~13,400 years BP (Aung-Thwin, 2001). In 2013, we conducted a 2.5 m-deep excavation at Badahlin Cave 2, which is separate from the site of Badahlin Cave 1 where the earlier excavations were undertaken. Gu Myaung Cave had not previously been excavated before 2013, when we conducted a 4 m-deep excavation. We collected three charcoal samples from the latter excavation, and these gave ^{14}C ages ranging from ~2,854 to ~15,261 years cal BP (see details in Tab. S3). The ^{14}C ages for Badahlin Cave 1 and Gu Myaung Cave provide preliminary—and likely minimum—age constraints for these two sites, which have yielded Palaeolithic artefacts. Additional data are needed to test these chronologies and extend them into the deeper deposits.

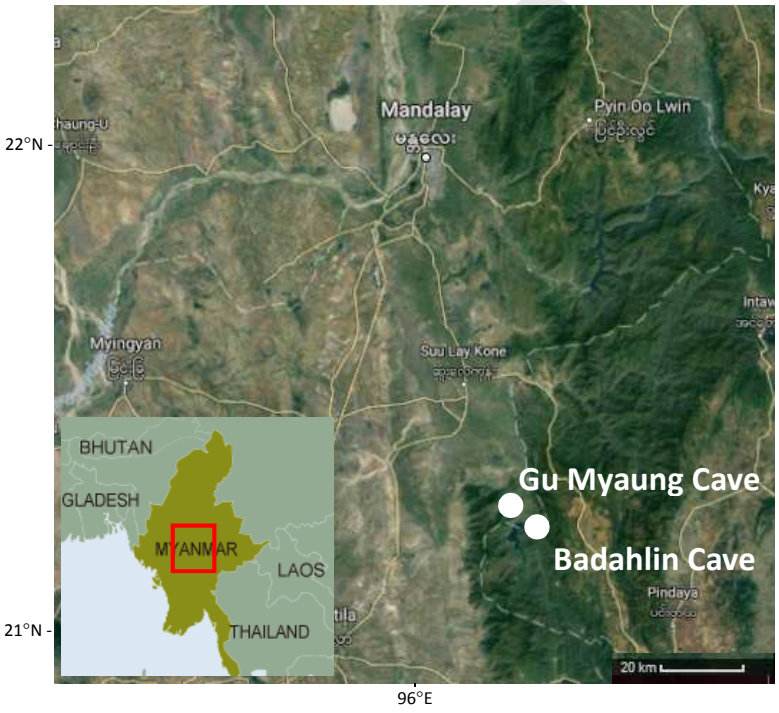

Figure 1. Map of central Myanmar showing the locations of both study sites.

Luminescence dating has been used previously to date archaeological sites in mainland Southeast Asia. Although conventional optically stimulated luminescence (OSL) dating of quartz has been applied to some sites (e.g., Demeter et al., 2015; Forestier et al., 2015; Moncel et al., 2016), the utility of quartz OSL is commonly limited due to signal saturation or low intrinsic brightness of OSL signals (Roberts et al., 2005; Jacobs and Roberts, 2007). We encountered these difficulties using the quartz OSL signal during our initial tests of the sediment samples collected from Badahlin and Gu Myaung Caves. Consequently, alternative minerals, luminescence signals and dating procedures require investigation. In this study, we have used two luminescence dating techniques—single-grain post-infrared infrared stimulated luminescence (pIRIR) and multi-grain infrared radiofluorescence (IR-RF)—both applied to sand-sized grains of potassium-rich feldspar (K-feldspar). Here we report the preliminary results of our investigations to augment the ^{14}C chronologies for these two human occupation sites. To our knowledge, these are the first luminescence ages for archaeological sites in Myanmar (Aung et al., 2015).

2 Site and sample descriptions

2.1 Study sites

Badahlin Cave (21.13274°N, 96.34032°E) and Gu Myaung Cave (21.20156°N, 96.31926°E) are located in central Myanmar (Fig. 1). They are formed in Permian and Permo-Triassic limestone, which contains a number of karstic features (e.g., sink holes, phreatic tubes).

Badahlin Cave was formed phreatically and consists of several inter-connecting chambers. The cave roof is ~30 m thick and speleothems are abundant, with occasional roof collapses facilitating entry routes for humans into the cave complex. We excavated a location close to the wall of one of the chambers to a depth of ~2.5 m (Fig. 2a); excavation details will be presented in a forthcoming archaeological report. The deposit is composed mainly of dark sandy silt that becomes enriched in clay with increasing depth; the sediment layers dip at a low angle towards the cave wall. The deposit is moist throughout, with a slight increase in moisture with depth. In

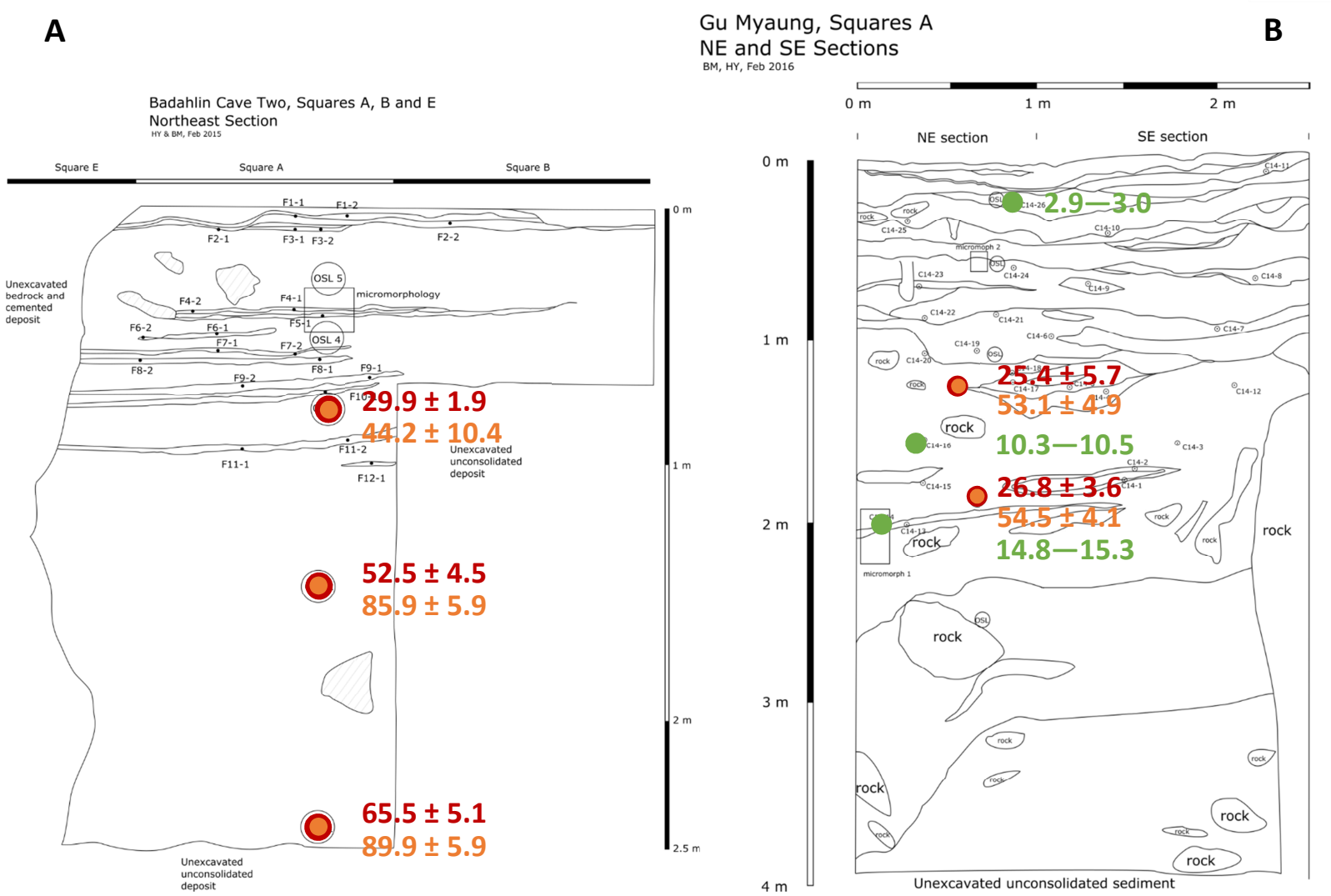

Figure 2. Section drawings of excavated sections at Badahlin Cave (A) and Gu Myaung Cave (B), showing pIRIR ages (red), IR-RF ages (IRSAR, orange) and calibrated ^{14}C age ranges (green). The pIRIR and IR-RF ages (± 1σ uncertainties) are in ka, and the ^{14}C age ranges (95.4% confidence interval) are in ka cal BP.

the upper part of the sequence (to a depth of ~1 m), the sediment layers are interspersed by thin flowstones. Calcified sediment and limestone inclusions were also found occasionally, the latter being usually cobble to pebble sized and irregularly shaped. Two excavations were undertaken: squares A, B and E relate to the first of these, and squares C and D to the second.

Gu Myaung Cave is also a phreatically formed limestone cave, which overlooks the Panlaung River. We excavated just inside the cave mouth to a depth of ~4 m (Fig. 2b); excavation details will be provided in an archaeological report currently being prepared. The upper 1.5 m of deposit consists mostly of horizontally layered sediment (grey-brown silt with some clay and pebbles), and hearth features with abundant white ash and charcoal. Boundaries between layers are well-defined, probably due to the short time since deposition and the lack of post-depositional disturbance. The number of hearth features declines below a depth of 1.5 m, resulting in a less heterogeneous and structured deposit. Below a depth ~2 m, no stratigraphic features are readily apparent, and the sediments are enriched with clay.

2.2 Sediment samples

The samples were collected using light-safe steel tubes, 22 cm in length and 5 cm in diameter. *In situ* measurements of the gamma-ray dose rate were made at each sample location by inserting a NaI(Tl) detector into the empty tube holes, and additional bags of sediment were collected from these holes for beta dose rate and moisture content measurements in the laboratory. Samples from Badahlin Cave were collected from relatively moist sediments in square A of the northeast section of the excavation, from 80, 150 and 240 cm depth below surface (Fig. 2a). Samples from Gu Myaung Cave were collected from the sediments (silty sand with some gravels) in the northeast section of the excavation, from 140 cm and 202 cm depth below surface (Fig. 2b). The uppermost sample at each site coincides with the depth of the lowest artefact found during excavation. The other samples were collected from the underlying archaeologically sterile layers and were analysed to investigate the longer-term depositional histories of these cave sites.

3 Methods

3.1 Sample preparation and instrumentation

Samples were prepared using standard methods—including wet-sieving, HCl acid and H_2O_2 treatments, and density separations—to isolate sand-sized grains (90–125 μm and 180–212 μm in diameter) of quartz and K-

feldspar. Our initial investigations of individual quartz grains (180–212 µm in diameter) revealed that their inherent OSL signals (i.e., their response to a test dose) were very weak or their natural OSL signals were in saturation. Accordingly, we concentrated thereafter on K-feldspar grains of the same or smaller (90–125 µm) grain size, isolating them using a sodium polytungstate solution with a density of 2.58 g/cm^3 and then etching them in 10% HF acid for 10 min to remove the alpha-dosed outer layer.

All pIRIR measurements were carried out on Risø TL/OSL-20 readers equipped with bialkali photomultiplier tubes (Electron Tubes Ltd 9235QB), blue-transmission filter packs (Schott BG 39 and Corning 7-59), infrared light-emitting diodes (LEDs), infrared lasers and calibrated ^{90}Sr/^{90}Y beta sources. Grains were loaded on to discs drilled with 100 holes, each 300 µm in depth and 300 µm in diameter, and each hole was calibrated for its beta dose rate. For relevant experiments, samples were bleached using an external solar simulator (Dr Hönle UVACUBE 400). The IR-RF measurements were performed on a Freiberg Instruments Lexsyg research reader equipped with a near-IR-sensitive photomultiplier tube (Hamamatsu H7421-50), a Chroma-D850/40 interference filter, a light source with different wavelengths (LEDs and IR laser, Richter et al., 2013) and a ^{90}Sr/^{90}Y beta source (Richter et al., 2012). The Lexsyg also has an in-built solar simulator (Richter et al., 2013), which we used for all bleaching steps during IR-RF measurements. All IR-RF measurements were performed on small aliquots ~2 mm in diameter, which consisted of ~70—230 grains in a single layer (dependent on grain size).

3.2 Environmental dose rates

Beta dose rates for dried and powdered sub-samples of the sediments collected in the field were measured using a Risø GM-25-5 beta counter (Bøtter-Jensen and Mejdahl, 1988) and the procedures described in Jacobs and Roberts (2015). The gamma dose rates were measured in the field using an Exploranium GR-320 EnviSpec gamma spectrometer, and the cosmic-ray dose rates were estimated following Prescott and Hutton (1994). Adjustments were made for beta-dose attenuation and for the effect of moisture content on the external beta, gamma and cosmic-ray dose rates; the measured (field) water contents were used for each sample and assigned an uncertainty of ± 25% (at 1σ) to accommodate any likely variations over the period of sample burial. The internal dose rate can be a significant contributor to the total dose rate for K-feldspar: we assumed an internal potassium content of 10 ± 2% (Smedley et al., 2012) and an internal Rb content of 400 ± 100 µg/g

(Huntley and Hancock, 2001), resulting in estimated internal dose rates of 0.38 ± 0.08 and 0.67 ± 0.12 Gy/ka for the 90–125 and 180–212 μm grains, respectively.

3.3 pIRIR measurement procedures

The pIRIR signal measured at elevated temperature has been reported to suffer much less from anomalous fading than the conventional infrared stimulated luminescence (IRSL) signal measured at 50°C, and to possibly not fade at all (e.g., Li and Li, 2011; J. P. Buylaert et al., 2012b; Li et al., 2014; Roberts et al., 2015). However, it is also harder to bleach in natural sunlight than either the IRSL signal or the quartz OSL signal (e.g., Li and Li, 2011; Colarossi et al., 2015). Single-grain measurements, therefore, provide a useful means of examining the extent of bleaching of individual grains in any particular sample and to check if significant post-depositional mixing has occurred (e.g., Reimann et al., 2012; Trauerstein et al., 2014; Blegen et al., 2015; Rhodes, 2015).

In this study, individual grains of K-feldspar were dated using a two-step single-grain pIRIR procedure (Blegen et al., 2015; details given in Table S1). In this procedure, the initial infrared stimulation is performed at 200°C for 100 s using infrared LEDs to stimulate all grains simultaneously; the pIRIR dating signals from individual grains are then measured at 275°C using a focused infrared laser beam for stimulation. A preheat of 320°C for 60 s was applied to the natural, regenerative and test doses; we used a test dose ~40% of the size of the expected natural dose. These parameters were chosen on the basis of dose recovery tests (Galbraith et al., 1999), as described below. To eliminate grains with luminescence properties unsuitable for the pIRIR procedure, we applied standard single-grain rejection criteria, following Blegen et al. (2015). Grains were rejected if: 1) the test dose signal measured during the natural dose cycle (T_n) was within 3σ of the background count; 2) the relative error on T_n exceeded 20%; 3) the 'recycling ratio' (i.e., the ratio between the sensitivity-corrected signals for a duplicate regenerative dose) was inconsistent with unity at 2σ; 4) the extent of 'recuperation' (i.e., the ratio between the sensitivity-corrected zero dose and natural dose signals) was greater than 5%; 5) the natural signal was equal to or higher than the saturation level of the dose response curve (DRC); and 6) the DRC could not be reliably fitted using a saturating exponential or an exponential-plus-linear function. For all accepted grains (i.e., those remaining after applying these rejection criteria), the equivalent dose (D_e) was estimated by projecting the sensitivity-corrected natural signal of each grain on to its corresponding sensitivity-corrected DRC.

3.4 IR-RF measurement procedures

Radioluminescence (RL) or radiofluorescence (RF) was first proposed as a dating technique in the late 1990s (Trautmann et al., 1998, 1999a) and recently revised by Frouin et al. (2017). The method is based on the fluorescence signal emitted during irradiation (Trautmann et al., 1999b), which has been suggested to not fade (Krbetschek et al., 2000; Novothny et al., 2010). If so, then the IR-RF signal would provide a validation test of the pIRIR results. In this study, we applied the original single-aliquot IR-RF procedure of Erfurt and Krbetschek (2003) and the updated procedure of Frouin et al. (2017) to multi-grain aliquots of K-feldspar for all samples.

Erfurt and Krbetschek's procedure—hereafter referred to as IRSAR—has four steps: 1) measure the natural IR-RF signal; 2) perform a prolonged solar bleach to reset the IR-RF signal; 3) wait for the superposing phosphorescence signal to decay; and 4) irradiate and measure the regenerated IR-RF signal (Table S1). All measurements made using the IRSAR procedure were carried out at room temperature. The revised IR-RF procedure proposed by Frouin et al. (2017)—hereafter referred to as RF_{70}—has a similar structure as the IRSAR procedure, but samples are measured and irradiated at an elevated temperature (70°C). To reach this temperature on the Lexsyg system, discs are required to be held at 70°C for 2 min before making IR-RF measurements. For both procedures, we adopted the solar bleach settings of Frouin et al. (2015) (Tab. S1).

The D_e value for each aliquot was obtained by sliding the regenerated IR-RF signal on to the natural IR-RF signal horizontally and vertically to minimise the residuals using the **R** function *analyse_IRSAR.RF()* in the **R** 'Luminescence' package (Kreutzer et al., 2017).

4 Results

4.1 Environmental dose rates

The total dose rates for all samples are summarised in Table 1, with the details given in Table S2. The total dose rates for samples from Badahlin Cave range from ~2.4 to ~3.9 Gy/ka, with much lower dose rates for the samples from Gu Myaung Cave (~1.3 Gy/ka). The dose rates are dominated by the beta dose rate (0.6–2.1 Gy/ka), with gamma dose rates of 0.3–1.3 Gy/ka, internal dose rates of 0.4–0.7 Gy/ka (depending on grain size) and cosmic-ray dose rates of 0.02 Gy/ka or less (the latter at Badahlin Cave because of rock shielding). The total dose rates for Badahlin Cave are two- or three-fold higher than for Gu Myaung Cave, which we attribute primarily to the greater amount of low-radioactivity carbonate in the latter samples. This is reflected in the U and Th concentrations measured by field gamma spectrometry, which differ significantly between the two

sites: ~ 5 μg/g U and ~7 μg/g Th at Badahlin Cave, compared to ~0.4 μg/g U and ~3.3 μg/g Th at Gu Myaung Cave.

4.2 Single-grain pIRIR

A representative single-grain pIRIR decay curve and DRC are shown for an accepted K-feldspar grain from sample BDL2-OSL 2 in Fig. S1. We conducted single-grain dose recovery tests on 3-5 discs of one sample of each site (BDL2-OSL 2 and GUMY-OSL 3) to validate the pIRIR experimental conditions used here for dating. Grains were bleached for 4 hr under the solar simulator to empty them of their natural doses, and then given a beta dose (as a surrogate natural dose) of ~236 Gy and ~30 Gy, respectively before being measured using the pIRIR procedure in Table S1. The weighted-mean dose recovery ratios (i.e., the ratio of measured to given doses) are 1.06 ± 0.04 and 0.97 ± 0.07, with dose overdispersion (OD) values of between 27% and 31% (Fig. S2). To examine the anomalous fading rate of the pIRIR signal, we estimated *g*-values for each sample using single (multi-grain) aliquots, following Auclair et al. (2003). The results obtained for storage periods of up to 2 weeks (Fig. S3) indicate that the *g*-values for the pIRIR signals are statistically consistent with zero (at 1σ) for all samples, which suggests that the pIRIR signals in these samples do not fade significantly, at least not on laboratory timescales. This finding is consistent with previous studies that have reported using an initial infrared stimulation at 200°C to effectively remove the fading component (e.g., Li and Li, 2012; Fu, 2014; Blegen et al., 2015; Yi et al., 2016).

The pIRIR signal has been shown to be relatively hard to bleach, with a residual dose of several Gy remaining even after prolonged bleaching in sunlight (Li and Li, 2011; Buylaert et al., 2012b). To determine and correct for any residual dose at the time of sediment deposition, we measured the dose values for 100—300 natural grains of each sample after bleaching them for 4 hr in the solar simulator. The weighted-mean residual dose for the Badahlin Cave samples is 7 ± 2 Gy and 0.01 ± 6 Gy for samples from Gu Myaung Cave. These residual doses are small to negligible compared with the measured D_e values of these samples, but we nonetheless subtracted them to estimate the final D_e values for age determination. In summary, the factors discussed above indicate that the pIRIR procedure is well-suited for our samples.

The D_e values were determined using 90–125 or 180–212 μm K-feldspar grains. The smaller grain size was used for two samples from Gu Myaung, owing to the scarcity of larger grains, and both grain-size fractions were measured for sample BDL2-OSL 3, as a methodological cross-check. The number of grains (or pseudo-single-

grain measurements for the 90–125 µm grains with ~5 grains per hole) that passed the rejection criteria corresponds to between 2% and 27% of the total number of grains measured (Table 1). Most of the grains were rejected based on the first criterion (low intrinsic brightness).

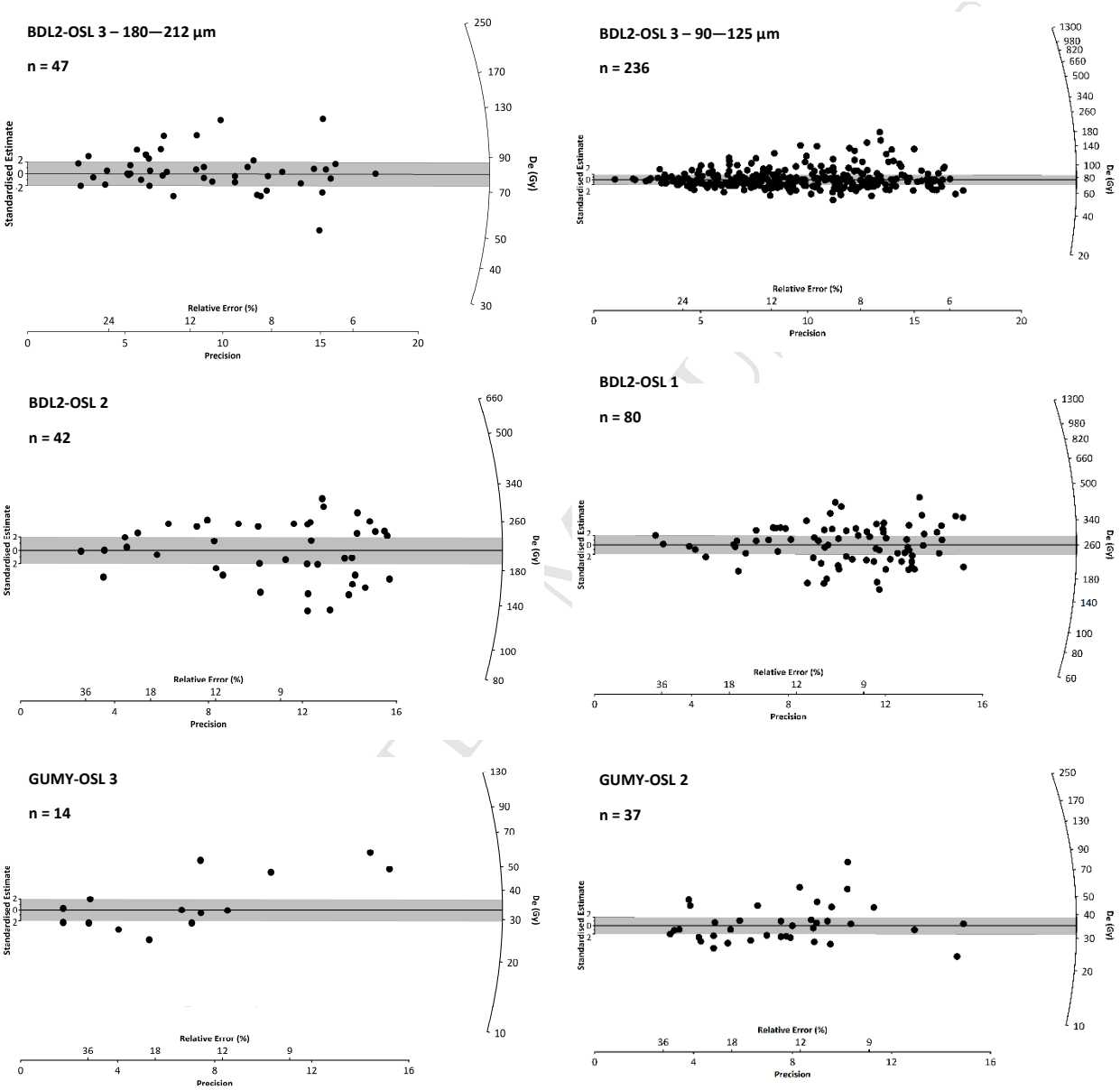

Figure 3. Single-grain pIRIR D_e-distribution of all samples shown as radial plots.

Fig. 3 shows pIRIR D_e distributions for all samples as radial plots. The datasets show some spread in D_e values, yielding OD values of 35-39% for the Badahlin samples and 61-70% for the Gu Myaung samples. A majority of the dispersion for the Badahlin samples, and a large portion of that for the Gu Myaung samples, can be

219 explained by a high overdispersion that arises from intrinsic factors, as suggested by the high overdispersion
220 values obtained in the dose recovery tests (27-31%, Fig. S2). The greater OD values for the samples from Gu
221 Myaung Cave may be due to beta microdosimetry variations, incomplete bleaching during the last sediment
222 transport event, or post-depositional mixing, but it is also notable that the D_e datasets for these two samples
223 are small, hence may result in inaccuracy in their OD estimation. The D_e datasets for most of the samples from
224 the two sites generally exhibit a symmetrical distribution (D_es randomly spread around a central value) and no
225 discrete D_e populations or leading edges at lower doses can be clearly identified, giving no indications of the
226 post-depositional mixing or partial bleaching issues. The only one exception is the 90-125 μm fraction of BDL2-
227 OSL 3 which exhibited some large outliers in its D_e dataset, but the D_e distribution of the 180-212 μm fraction
228 of the same sample doesn't seem to suggest any partial bleaching problem, and the weighted mean ages of
229 these two fractions are indistinguishable from each other (Table 1).

230 Based on these observations, in the current stage we calculated the D_e values for all samples using the central
231 age model (CAM), which gives an estimate of the weighted geometric mean (Galbraith et al., 1999; Galbraith
232 and Roberts, 2012). The final ages are shown in Table 1. The ages for the three samples from Badahlin Cave
233 range from ~30 to ~66 ka and are in stratigraphic order, while the two samples from Gu Myaung Cave are both
234 terminal Pleistocene in age (~25—27 ka).

235 *Table 1: D_e values, dose rates and calculated pIRIR and IR-RF ages for all samples. CAM D_e values were calculated for all pIRIR and IR-RF samples. The pIRIR*
236 *D_e values were corrected for a small residual dose (see text). For IR-RF D_e estimation, only 2-5 single-aliquots per sample were measured (both protocols).*

Sample	Depth [cm]	Grain size [µm]	n[1]	Dose rate [Gy/ka]	Equivalent dose [Gy]			OD [%]	Age [ka]		
					pIRIR (CAM)	IR-RF (IRSAR)	IR-RF (RF_{70})		pIRIR (CAM)	IR-RF (IRSAR)	IR-RF (RF_{70})
BDL2-OSL 3	80	90–125	1200/326	2.38 ± 0.13	71 ± 2	105 ± 24	129 ± 8	38 ± 2	29.9 ± 1.9	44.2 ± 10.4	54.3 ± 4.6
		180–212	300/47	2.60 ± 0.16	80 ± 3	-	-	35 ± 4	30.8 ± 2.3	-	-
BDL2-OSL 2	150	180–212	300/42	3.86 ± 0.20	203 ± 13	332 ± 13	343 ± 26	38 ± 5	52.5 ± 4.5	85.9 ± 5.9	88.8 ± 8.4
BDL2-OSL 1	240	180–212	300/80	3.85 ± 0.23	252 ± 12	346 ± 8	281 ± 13	39 ± 3	65.5 ± 5.1	89.9 ± 5.9	73.0 ± 5.6
GUMY-OSL 3	140	90–125	600/14	1.31 ± 0.10	33 ± 7	69 ± 4	93 ± 29	70 ± 15	25.4 ± 5.7	53.1 ± 4.9	59.9 ± 19.4
GUMY-OSL 2	202	90–125	600/37	1.31 ± 0.09	35 ± 4	71 ± 2	-	61 ± 8	26.8 ± 3.6	54.5 ± 4.1	-

237 [1] Grains (measured/ accepted)

4.3 Multi-grain IR-RF

Before determining D_e values using the IRSAR IR-RF procedure, we conducted several tests to determine the most appropriate measurement conditions. Previous studies have suggested that prolonged solar bleaching (step 2 in Table S1) is required in the procedure to reset the IR-RF signal (e.g., 3 hr: Frouin et al., 2015, 2017). For our samples, however, we found that solar simulator bleaches of >1 hr did not cause further increase in the IR-RF signal (i.e. the source traps of IR-RF have been fully emptied by 1 hr solar simulator bleach) (Fig. 4, left panel), so we used a solar bleach time of 1 hr in this study. We also performed a pause duration test to determine the minimum delay time needed to eliminate phosphorescence before measuring the regenerated IR-RF signal (step 3 in Table S1). We found that, similar to Buylaert et al. (2012a), the phosphorescence signals of our samples are very weak compared to the IR-RF signal (Fig. S4), and we could not distinguish between the regenerated IR-RF signals measured after pauses of 15 to 60 min (Fig. 4, right panel). We concluded, therefore, that the effects of phosphorescence on the IR-RF signals of our samples are negligible after a pause time of 15 min, which we adopted to save machine time. We caution, however, that these settings are sample- and instrument-specific and may not be appropriate for samples from other sites. To validate our revised procedures, we conducted dose recovery tests on natural aliquots of samples BDL2-OSL 3 (Fig. S5) and GUMY-OSL 3 after bleaching them for 4 h in the solar simulator and giving them beta doses similar to their expected D_e values. The weighted-mean dose recovery ratios are 1.06 ± 0.03 and 1.31 ± 0.13, respectively, suggesting the given dose can be recovered with sufficient accuracy using the experimental conditions in our IRSAR procedure (Table S1) for samples from Badahlin cave, and will be slightly overestimated for samples from Gu Myaung cave.

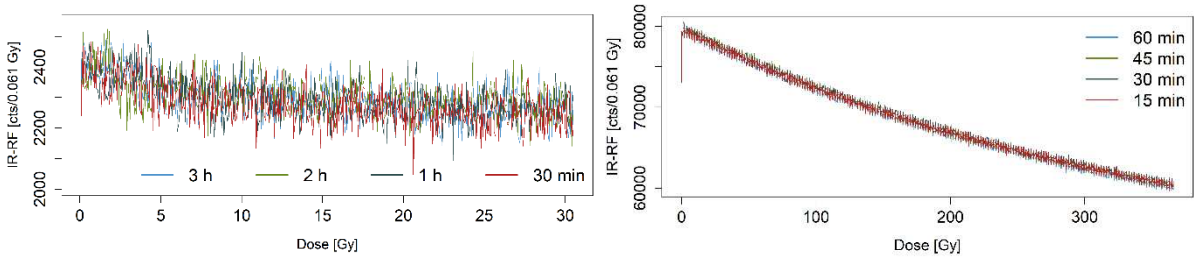

Figure 4. A test of solar bleaching time (left) and pause time (right) for IR-RF measurements of sample BDL2-OSL 3. The IRSAR protocol was used as described in Table S1. In the first experiment (left panel), one used disc of the sample was given a regenerative dose of ~305 Gy, bleached for a

duration of t_b using the solar simulator equipped in the Lexsyg reader, and paused for one hour before the IR-RF signal being measured. This cycle was repeated four times with t_b varied from 30 mins to 3 hours. The left panel only shows an early portion (0—30 Gy) of the IR-RF signal; in the second experiment (right panel), in each cycle the same disc was first bleached for one hour using the solar simulator and pause for a duration of t_p before the IR-RF signal being measured. This cycle was repeated four times with t_p varied from 15 mins to 60 mins. More results are given in Fig. S4.

We also tested the RF_{70} procedure (Frouin et al., 2017) on our samples. Preliminary tests showed that IR-RF measurements made at 70°C did not improve the decay curve shapes for our samples, in contrast to those of Huot et al. (2015) and Frouin et al. (2017). Nevertheless, the RF_{70} procedure yields slightly different results to those obtained using the IRSAR procedure: the IR-RF signal intensity is higher and the calculated D_e values differ by between ~10 and ~65 Gy (Fig. 5). The cause(s) of these differences are under investigation, including tests of the suitability of the RF_{70} measurement conditions for our samples.

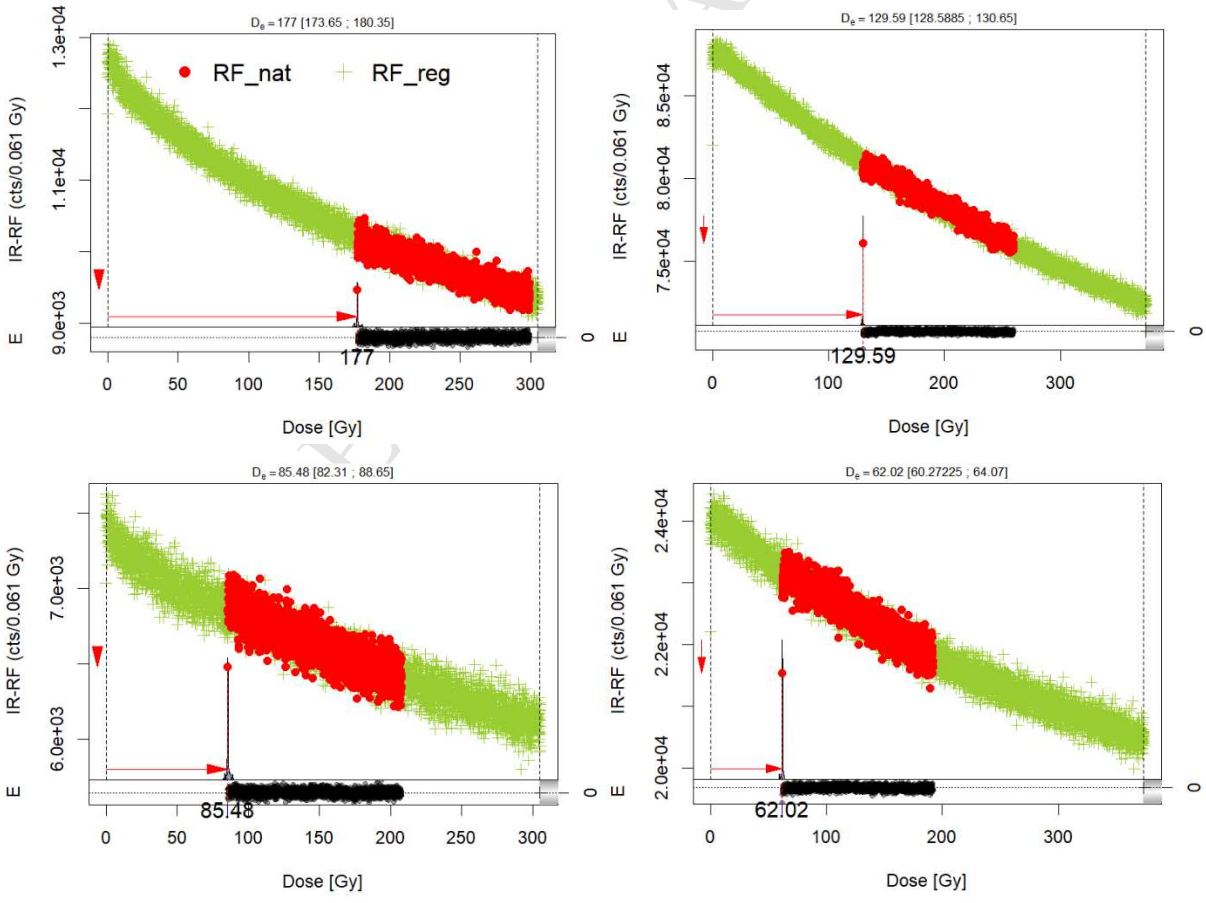

Figure 5: IRSAR and RF_{70} data for sample BDL2-OSL 3 from Badahlin Cave (top panels) and sample GUMY-OSL 3 from Gu Myaung Cave (bottom panels). The D_e values are ~177 Gy (top left) and ~85 Gy (bottom left) for IRSAR, and ~130 Gy (top right) and ~62 Gy (bottom right) for RF_{70}.

We estimated the IR-RF ages by calculating weighted-mean D_e values using the CAM (Table 1), although only 2-5 single-aliquots were measured for each sample. We did not subtract any residual doses from the measured D_e values, and are currently in the process of assessing their likely size. The CAM ages range from ~44 to 90 ka (IRSAR) and ~54 to 89 ka (RF_{70}) at Badahlin Cave, and both samples from Gu Myaung Cave yielding ages of ~54 ka (IRSAR) and ~60 ka (RF_{70}, only GUMY-OSL 3) (Tab. 1). All of these ages are much older than the pIRIR and ^{14}C chronologies, which is inferred to due to insufficient bleaching of the IR-RF signal. Subtraction of appropriate residual doses would likely reduce these age discrepancies considerably.

5 Discussion

In this preliminary study of K-feldspar grains from two archaeological sites in central Myanmar, we have shown that the single-grain pIRIR procedure is suitable for dating, with acceptable results from dose recovery tests and no evidence for fading of the pIRIR signal over laboratory timescales. There is potential, therefore, to extend the applicability of pIRIR dating to other Palaeolithic sites in mainland Southeast Asia.

A comparison with independent (^{14}C) age control at Gu Myaung Cave has revealed, however, that the pIRIR CAM ages (~25—27 ka) overestimate the ^{14}C ages (~10 and ~15 ka cal BP, Tab. S3) obtained for charcoal fragments collected from stratigraphic layers between and below these two sediment samples (Fig. 2b). Currently, there is no further evidence to validate either of these two chronologies. The residual dose test suggested that the pIRIR signal for these K-feldspar grains can be (nearly) fully reset by mimic sunlight bleaching in the laboratory. The D_e distribution patterns of the two samples from the Gu Myaung Cave provide no clear evidence for partial bleaching. Therefore, the causes of this discrepancy in age are still under investigation. Further investigations on the residual doses of both sites will be carried out on very young samples from the upper part of the stratigraphy. This will give us an implication about whether the pIRIR residual doses measured in the lab are representative for the natural sediment. The reliability of the radiocarbon ages in these sites also warrant further test, by comparing with more chronologies derived from other dating techniques (such as U-series dating).

The IR-RF ages obtained in this study overestimate their pIRIR counterparts by around 25 ka (Tab. 1), which we attribute to the different bleachabilities of these two signals, together with the use of multiple grains for IR-RF dating, which will exacerbate problems of D_e overestimation due to partial bleaching. We note a common pattern to the pIRIR and IRSAR IR-RF ages: each set of ages increases with depth at Badahlin Cave, while the two pIRIR ages for Gu Myaung Cave are statistically indistinguishable, as are the two IR-RF ages (IRSAR). This suggests a systematic underlying cause for the age offset, which we are currently investigating. Other future lines of enquiry include further testing of the RF_{70} procedure of Frouin et al. (2017), including dose recovery tests and other variations to readout temperature and processing younger samples from both sites to get a better estimate of the residual dose.

Based on our dating results for Badahlin Cave, occupation started at least ~30 ka ago during Marine Isotope Stage (MIS) 2 or possibly MIS 3 (Fig.2a). The underlying, culturally sterile deposits dated to ~53 and ~66 ka might be interpreted as evidence that people had not arrived in this region by 53 ka, but we consider such inferences as premature given the many chambers yet to be excavated. Sediments have been accumulating in parts of the large cave complex for more than 50 millennia and further excavations may reveal earlier traces of human habitation. Occupation of Gu Myaung Cave, based on our current ages, appears to have commenced ~25 ka ago, close to the Late Pleistocene–Holocene transition (Fig. 2b). Again, however, a longer record of human occupation cannot be ruled out on the basis of the limited excavations conducted thus far at this site.

6 Conclusions

We have applied single-grain pIRIR and multi-grain IR-RF dating procedures to K-feldspar extracts from archaeological deposits at Badahlin and Gu Myaung Caves in central Myanmar. Luminescence investigations of the pIRIR and IR-RF signals and D_e distributions, indicates that the pIRIR procedure, at least, may be suitable for sediment dating. The IR-RF ages overestimate the pIRIR D_e values and ages by a considerable margin, which may be related to the poorer bleachability and higher residual doses associated with the IR-IF signal. Future investigations could involve IR-RF measurements of individual K-feldspar grains (e.g., Trautmann et al., 2000) to avoid the shortcomings of using multi-grain aliquots to date partially bleached sediments. Our preliminary pIRIR chronologies indicate that human occupation of Badahlin and Gu Myaung Caves started at least ~30 and ~25 ka ago, respectively, thereby adding to the sparse chronological record supporting Palaeolithic settlement of the region during the Late Pleistocene (Aung et al., 2015).

Acknowledgements

This study is funded by the Australian Research Council through Future Fellowships to B.L. (FT140100384) and B.M. (FT140100101) and an Australian Laureate Fellowship to R.G.R. (FL130100116), and by the University of Wollongong through a Postgraduate Award and an International Postgraduate Research Scholarship to M.S. We would like to acknowledge the financial support by the "PalaeoChron" project awarded to Prof. Tom Higham by the European Research Council under the European Union's Seventh Framework Programme (FP7/2007-2013)/ ERC grant agreement no. 324139. We would also like to thank Zaw Phyo, Tin Thut Aung, May Su Ko, Hu Yue, Myo Thi Ha and Yin Min for assisting with the excavations, and the teams in the luminescence laboratories at the University of Wollongong (Australia) and the University of Bayreuth (Germany) for assisting with sample preparation and measurement.

346 **References**

347 Auclair, M., Lamothe, M., Huot, S., 2003. Measurement of anomalous fading for feldspar IRSL using SAR.
348 Radiat. Meas. 37, 487–492. doi:10.1016/S1350-4487(03)00018-0

349 Aung-Thwin, M., 2001. Origins and Development of the Field of Prehistory in Burma. Asian Perspect. 40, 6–34.
350 doi:10.1353/asi.2001.0002

351 Aung, T.H., Marwick, B., Conrad, C., 2015. Palaeolithic Zooarchaeology in Myanmar: A Review and Future
352 Prospects. J. Indo-Pacific Archaeol. 39, 50–56. doi:10.7152/jipa.v39i0.14896

353 Aung Thaw, U., 1971. The "Neolithic" Culture of the Padah-lin Caves. Asian Perspect. 14, 123–133.

354 Blegen, N., Tryon, C.A., Faith, J.T., Peppe, D.J., Beverly, E.J., Li, B., Jacobs, Z., 2015. Distal tephras of the eastern
355 Lake Victoria basin, equatorial East Africa: Correlations, chronology and a context for early modern
356 humans. Quat. Sci. Rev. 122, 89–111. doi:10.1016/j.quascirev.2015.04.024

357 Bøtter-Jensen, L., Mejdahl, V., 1988. Assessment of beta dose rate using a GM multicounter system. Nucl.
358 Tracks Radiat. Meas. 14, 187–191. doi:10.1016/1359-0189(88)90062-3

359 Buylaert, J.P., Jain, M., Murray, A.S., Thomsen, K.J., Lapp, T., 2012. IR-RF dating of sand-sized K-feldspar
360 extracts: A test of accuracy. Radiat. Meas. 47, 759–765. doi:10.1016/j.radmeas.2012.06.021

361 Buylaert, J.P., Jain, M., Murray, A.S., Thomsen, K.J., Thiel, C., Sohbati, R., 2012. A robust feldspar luminescence
362 dating method for Middle and Late Pleistocene sediments. Boreas 41, 435–451. doi:10.1111/j.1502-
363 3885.2012.00248.x

364 Colarossi, D., Duller, G.A.T., Roberts, H.M., Tooth, S., Lyons, R., 2015. Comparison of paired quartz OSL and
365 feldspar post-IR IRSL dose distributions in poorly bleached fluvial sediments from South Africa. Quat.
366 Geochronol. 30, 233–238. doi:10.1016/j.quageo.2015.02.015

367 Demeter, F., Shackelford, L., Westaway, K., Duringer, P., Bacon, A.M., Ponche, J.L., Wu, X., Sayavongkhamdy,
368 T., Zhao, J.X., Barnes, L., Boyon, M., Sichanthongtip, P., Sénégas, F., Karpoff, A.M., Patole-Edoumba, E.,
369 Coppens, Y., Braga, J., 2015. Early Modern humans and morphological variation in Southeast Asia:Fossil
370 evidence from tam pa ling, laos. PLoS One 10, 1–17. doi:10.1371/journal.pone.0121193

371 Erfurt, G., Krbetschek, M.R., 2003. IRSAR–A single-aliquot regenerative-dose dating protocol applied to the

372 infrared radiofluorescence (IR-RF) of coarse-grain K feldspar. Anc. TL 21, 35–42.

373 Forestier, H., Sophady, H., Puaud, S., Celiberti, V., Frere, S., Zeitoun, V., Mourer-Chauvire, C., Mourer, R., Than,
374 H., Billault, L., 2015. The Hoabinhian from Laang Spean Cave in its stratigraphic, chronological, typo-
375 technological and environmental context (Cambodia, Battambang province). J. Archaeol. Sci. Reports 3,
376 194–206. doi:10.1016/j.jasrep.2015.06.008

377 Frouin, M., Huot, S., Kreutzer, S., Lahaye, C., Lamothe, M., Philippe, A., Mercier, N., 2017. An improved
378 radiofluorescence single-aliquot regenerative dose protocol for K-feldspars. Quat. Geochronol. 38, 13–
379 24. doi:10.1016/j.quageo.2016.11.004

380 Frouin, M., Huot, S., Mercier, N., Lahaye, C., Lamothe, M., 2015. The issue of laboratory bleaching in the
381 infrared-radio fluorescence dating method. Radiat. Meas. 81, 212–217.
382 doi:10.1016/j.radmeas.2014.12.012

383 Fu, X., 2014. The D e (T, t) plot: A straightforward self-diagnose tool for post-IR IRSL dating procedures.
384 Geochronometria 41, 315–326. doi:10.2478/s13386-013-0167-9

385 Galbraith, R.F., Roberts, R.G., 2012. Statistical aspects of equivalent dose and error calculation and display in
386 OSL dating: An overview and some recommendations. Quat. Geochronol. 11, 1–27.
387 doi:10.1016/j.quageo.2012.04.020

388 Galbraith, R.F., Roberts, R.G., Laslett, G.M., Yoshida, H., Olley, J.M., 1999. Optical Dating of Single and Multiple
389 Grains of Quartz From Jinmium Rock Shelter, Northern Australia: Part I, Experimental Design and
390 Statistical Models. Archaeometry 41, 339–364. doi:10.1111/j.1475-4754.1999.tb00987.x

391 Huntley, D.J., Hancock, R.G. V., 2001. The Rb contents of the K-feldspar grains being measured in optical
392 dating. Anc. TL 19, 43–46.

393 Huot, S., Frouin, M., Lamothe, M., 2015. Evidence of shallow TL peak contributions in infrared
394 radiofluorescence. Radiat. Meas. 81, 237–241. doi:10.1016/j.radmeas.2015.05.009

395 Jacobs, Z., Roberts, R.G., 2015. An improved single grain OSL chronology for the sedimentary deposits from
396 Diepkloof Rockshelter, Western Cape, South Africa. J. Archaeol. Sci. 63, 175–192.
397 doi:10.1016/j.jas.2015.01.023

398 Jacobs, Z., Roberts, R.G., 2007. Advances in optically stimulated luminescence dating of individual grains of
399 quartz from archeological deposits. Evol. Anthropol. 16, 210–223. doi:10.1002/evan.20150

400 Krbetschek, M.R., Trautmann, T., Dietrich, A., Stolz, W., 2000. Radioluminescence dating of sediments:
401 methodological aspects. Radiat. Meas. 32, 493–498. doi:10.1016/S1350-4487(00)00122-0

402 Kreutzer, S., Dietze, M., Burow, C., Fuchs, M.C., Schmidt, C., Fischer, M., Friedrich, J., Mercier, N., Smedley,
403 R.K., Christophe, C., Zink, A., Durcan, J., King, G., Philippe, A., Guerin, G., Fuchs, 2017. Comprehensive
404 Luminescence Dating Data Analysis.

405 Li, B., Li, S.-H., 2012. A reply to the comments by Thomsen et al . on " Luminescence dating of K-feldspar from
406 sediments : a protocol without anomalous fading correction " 8, 49–51.
407 doi:10.1016/j.quageo.2011.10.001

408 Li, B., Li, S.H., 2011. Luminescence dating of K-feldspar from sediments: A protocol without anomalous fading
409 correction. Quat. Geochronol. 6, 468–479. doi:10.1016/j.quageo.2011.05.001

410 Li, B., Roberts, R.G., Jacobs, Z., Li, S.-H., 2014. A single-aliquot luminescence dating procedure for K-feldspar
411 based on the dose-dependent MET- pIRIR signal sensitivity. Quat. Geochronol. 20, 51–64.
412 doi:10.1016/j.quageo.2013.11.001

413 Moncel, M.-H., Arzarello, M., Boëda, É., Bonilauri, S., Chevrier, B., Gaillard, C., Forestier, H., Yinghua, L., Sémah,
414 F., Zeitoun, V., 2016. Assemblages with bifacial tools in Eurasia (second part). What is going on in the
415 East? Data from India, Eastern Asia and Southeast Asia. Comptes Rendus Palevol.
416 doi:http://dx.doi.org/10.1016/j.crpv.2015.09.010

417 Novothny, A., Frechen, M., Horvath, E., Krbetschek, M.R., Tsukamoto, S., 2010. Infrared stimulated
418 luminescence and radiofluorescence dating of aeolian sediments from Hungary. Quat. Geochronol. 5,
419 114–119. doi:10.1016/j.quageo.2009.05.002

420 Prescott, J.R., Hutton, J.T., 1994. Cosmic ray contributions to dose rates for luminescence and ESR dating: Large
421 depths and long-term time variations. Radiat. Meas. 23, 497–500. doi:10.1016/1350-4487(94)90086-8

422 Reimann, T., Thomsen, K.J., Jain, M., Murray, A.S., Frechen, M., 2012. Single-grain dating of young sediments
423 using the pIRIR signal from feldspar. Quat. Geochronol. 11, 28–41. doi:10.1016/j.quageo.2012.04.016

Rhodes, E.J., 2015. Dating sediments using potassium feldspar single-grain IRSL: Initial methodological considerations. Quat. Int. 362, 14–22. doi:10.1016/j.quaint.2014.12.012

Richter, D., Pintaske, R., Dornich, K., Krbetscheck, M., 2012. A novel beta source design for uniform irradiation in dosimetric applications. Anc. TL 30, 57–64.

Richter, D., Richter, A., Dornich, K., 2013. Lexsyg — A new system for luminescence research. Geochronometria 40, 220–228. doi:10.2478/s13386-013-0110-0

Roberts, R.G., Li, B., Jacobs, Z., Jankowski, N., Cunningham, A.C., 2015. Optical dating in archaeology : thirty years in retrospect and grand challenges for the future. J. Archaeol. Sci. 56, 41–60. doi:10.1016/j.jas.2015.02.028

Roberts, R.G., Morwood, M.J., Westaway, K.E., 2005. Illuminating Southeast Asian Prehistory: New Archaeological and Paleoanthropological Frontiers for Luminescence Dating. Asian Perspect. 44, 293–319. doi:10.1353/asi.2005.0028

Smedley, R.K., Duller, G.A.T., Pearce, N.J.G., Roberts, H.M., 2012. Determining the K-content of single-grains of feldspar for luminescence dating. Radiat. Meas. 47, 790–796. doi:10.1016/j.radmeas.2012.01.014

Trauerstein, M., Lowick, S.E., Preusser, F., Schlunegger, F., 2014. Small aliquot and single grain IRSL and post-IR IRSL dating of fluvial and alluvial sediments from the Pativilca valley, Peru. Quat. Geochronol. 22, 163–174. doi:10.1016/j.quageo.2013.12.004

Trautmann, T., Dietrich, A., Stolz, W., Krbetschek, M.R., 1999a. Radioluminescence dating: A new tool for quaternary geology and archaeology. Naturwissenschaften 86, 441–444. doi:10.1007/s001140050649

Trautmann, T., Krbetschek, M.R., Dietrich, A., Stolz, W., 1999b. Feldspar radioluminescence: a new dating method and its physical background. J. Lumin. 85, 45–58. doi:10.1016/S0022-2313(99)00152-0

Trautmann, T., Krbetschek, M.R., Dietrich, A., Stolz, W., 1998. Investigations of feldspar radioluminescence: potential for a new dating technique. Radiat. Meas. 29, 421–425. doi:10.1016/S1350-4487(98)00012-2

Yi, S., Buylaert, J.P., Murray, A.S., Lu, H., Thiel, C., Zeng, L., 2016. A detailed post-IR IRSL dating study of the Niuyangzigou loess site in northeastern China. Boreas 45, 644–657. doi:10.1111/bor.12185